Scaling of spin-echo amplitudes with frequency, diffusion coefficient, pore size, and susceptibility difference for the NMR of fluids in porous media and biological tissues

Giulio C. Borgia,[1] Robert J. S. Brown,[2] and Paola Fantazzini[3]
[1]*Istituto di Scienze Minerarie, Università di Bologna, Viale Risorgimento 2, 40136 Bologna, Italy*
[2]*515 West 11th Street, Claremont, California 91711-3721*
[3]*Dipartimento di Fisica, Università di Bologna, Via Irnerio 46, 40126 Bologna, Italy*
(Received 26 September 1994)

Both Carr-Purcell-Meiboom-Gill (CPMG) measurements and single-spin-echo measurements have been made at frequencies of $\nu=10$, 20, and 50 MHz for two relatively homogeneous porous porcelain materials with different pore sizes, both saturated separately with three liquids of different diffusion coefficients. The CPMG transverse relaxation rate is increased by an amount R by diffusion in the inhomogeneous fields caused by susceptibility differences χ; R shows the dependence on τ (half the echo spacing) given by the model of Brown and Fantazzini [Phys. Rev. B **47**, 14 823 (1993)] if relaxation is slow enough that there are several CPMG echoes in a transverse relaxation time. For τ values over a range of a factor of about 40, the increase of R with τ is nearly linear, with a slope that is independent of pore dimension a and diffusion coefficient D. For this nearly linear region and a short initial region quadratic in τ, we find $R \propto (\chi\nu)^2$. In these regions we can scale and compare measurements of R taken for different values of χ ν, a, and D by plotting $RD/(\frac{1}{3}\chi\nu a)^2$ vs $D\tau/a^2$. The asymptotic values of R for large τ for CPMG data can be inferred from the asymptotic *slope*, $-R_s$, of $\ln M$ (magnetization) for single spin echoes as a function of echo time $t=2\tau$. It is shown from the Bloch-Torrey equations for NMR with diffusion that, for any combination of parameters χ, ν, a, or D, the magnetization M is a function of both a dimensionless time (either $t_u=Dt/a^2$ or $t_v-\frac{1}{3}\chi\nu t$) and a dimensionless parameter $\xi=\frac{1}{3}\chi\nu a^2/D$. If $\xi<2$ (for our particular porous media and definition of the distance a), the asymptotic slope of $-\ln M$ is approximately $R_s=\frac{1}{3}\chi\nu$, that is, it is proportional to only the first power of $\chi\nu$ and does not depend on either a or D. These results are compatible with the existence of a long-tailed distribution of phases, such as a truncated Cauchy distribution, at echo time. Diffusion does not lead to a reduction of R_s because averages of choices from a Cauchy distribution give the same distribution rather than a narrower one as for the Gaussian distribution. For larger ξ the decay of $\ln M$ decreases and no longer approaches a linear asymptote during measurement times. A semiempirical expression for the large-ξ case is given. These scaling laws should help in predicting the effects of changes in frequency and of susceptibility contrast as well as of changes in temperature, fluid, or range of pore sizes or other characteristic dimensions.

PACS number(s): 47.55.Mh, 66.10.−x, 76.60.Lz, 76.60.Es

I. INTRODUCTION

As is well known [1], measurements of the transverse relaxation time T_2 are affected by diffusion if inhomogeneous magnetic fields are present. Carr-Purcell-Meiboom-Gill [2,3] (CPMG) measurements can reduce the effects of diffusion on T_2, but the results depend on τ, half the echo spacing. When the fields are inhomogeneous over sample or instrument dimensions, it is often possible to make τ short enough to substantially eliminate diffusion effects. In porous media, including biological tissues, there are often inhomogeneous fields due to magnetic susceptibility differences, with substantial change of field over distances of the order of pore dimensions. Especially at high measurement frequencies it may not be possible to make τ short enough to eliminate diffusion effects. Although these diffusion effects are often a nuisance to be overcome, they can also be a source of information on such parameters as pore dimensions or be a source of contrast [4] in medical magnetic resonance imaging (MRI). Susceptibility differences may be intentionally introduced by manipulating the susceptibility of any phase of the porous medium or by introducing magnetic particles [5,6].

Several groups [4,7,8] have made Monte Carlo computations of signal decay for gradient echoes, Hahn spin echoes, or CPMG echo trains for systems with diffusion through short-distance-scale inhomogeneous fields, and in one case [4] the Bloch-Torrey [9] equations for NMR with diffusion have been used to generalize the results of the computations. It has been noted [10] that, for CPMG measurements in some porous media, the T_2^{-1} vs τ curve has a substantial portion that is nearly linear. Brown and Fantazzini [11,12] (references to be referred to as I and II, respectively) have presented a heuristic model that accounts for this nearly linear portion in terms of a distribution of correlation times τ_{ci} for change of precession frequency resulting from diffusion in local fields due to susceptibility differences. The papers I and II provide useful background for the present work, as do various references [13–23] therein. We will show that the correlation times can be scaled for changes of diffusion coefficient or for a linear scaling up or down of the di-

mensions in the structure of the porous medium.

It is useful both in designing and interpreting measurements to know how R (rate difference, R_d in I and II), which is defined as the contribution to T_2^{-1} of diffusion through local inhomogeneous fields, varies with frequency ν, diffusion coefficient D, characteristic dimension of pore space a, and susceptibility difference χ between components of the medium. Kleinberg, Farooqui, and Horsfield [24] have shown that T_2 data showing surface effects in porous media are easier to interpret when the data are taken at low frequencies, where the effects of susceptibility differences are reduced. Several new NMR logging instruments for oil wells operate at frequencies of 1 or 2 MHz [25,26].

It will be seen generally that magnetization decay caused by diffusion in inhomogeneous fields due to susceptibility differences depends only on a diffusion time a^2/D and a dephasing rate $\frac{1}{3}\chi\nu$ in addition to echo time for a given spin-echo measurement sequence and the *shape* of the given pore space. The product ξ of this diffusion time and dephasing rate will be a useful parameter for identifying regions of different behavior of the echo decay.

Both to show the general dependence of R on the parameters and for help in interpreting data taken in one regime for use in another, scaling laws will be developed, and both CPMG and Hahn single-echo measurements of T_2^{-1} at three frequencies, with three liquids with different diffusion coefficients, and in two relatively uniform porous media, will be presented to illustrate the scaling.

II. THEORY

In I ω is defined as the difference between the local precession frequency, as influenced by the susceptibility contrast of a porous medium, and the mean frequency ω_0 for each spin in a region of the pore system which is somewhat larger than the spin can diffuse through in measurement times. We will follow the effects on T_2^{-1} of the diffusion through these frequency differences and see how these effects depend on the susceptibility difference χ between the pore fluid and the solid matrix (or equivalent in the case of biological tissues), the measurement frequency ν, the diffusion coefficient D, and a characteristic length a of a porous medium to be scaled up or down in dimensions without changing the shape of the pore space. The length a may be defined or measured in any consistent manner for the porous media to be scaled.

It will be necessary to define a number of variables, some of them both as dimensional quantities and also in three different dimensionless forms. In all cases the subscript u (possibly following other subscripts) will indicate that all time variables (including those in differential operators, rates, or frequencies) are in units of a^2/D. The subscript v will always indicate that times are in units of $(\frac{1}{3}\chi\nu)^{-1}$, and w will always indicate that times are in units of $D(\frac{1}{3}\chi\nu a)^{-2}$. In all three cases all distances are in units of a. The coefficient $\frac{1}{3}$ was chosen to give, for our data, approximate unit value to a dimensionless rate R_{sv} to be defined later. The length a can be any characteristic length of a pore system which may, at least conceptually, be scaled up or down in size. It is the measured effective pore entrance radius for the present samples. We define the dimensionless ratio $\xi=\tau_u/\tau_v=\frac{1}{3}\chi\nu a^2/D$ and note that the time units for subscripts u, v, and w are in ratios $1:\xi^{-1}:\xi^{-2}$, and we will see that for $\xi\gtrsim 2$ the behavior of single spin echoes deviates from that for smaller ξ. It should be clear that the value of ξ depends on how the characteristic length a is defined or measured and on the nature and complexity of the porous medium. Thus statements about behavior in certain ξ ranges, e.g., $\xi\gtrsim 2$, are likely to need to be adapted to individual measurement systems, depending on the definition or measurement of a.

The symbol R will be used for values of $1/T_2(\tau)-1/T_2(\tau\rightarrow 0)$ from CPMG measurements. The 90° pulse time τ is half the echo spacing for CPMG measurements or half the echo time t for single-echo measurements. Continuous time variables will also be called t, but the context will make this clear. The asymptotic slope of $-\ln M$ (magnetization, echo amplitude) as a function of t for single-echo curves will be called R_s (for single echo). Also, the quantities T_3, T_4, and T_5 will be defined. In all of these cases the subscripts u, v, or w may be added with the meaning given above.

A. Scaling the Bloch-Torrey equations

We next note that ω is a function of $\mathbf{r}/a$ which does not depend on the scale length a. To see this we note that ω comes from local fields due to volume magnetization in the solid framework of the porous medium and that dipole fields are inversely proportional to distance cubed, namely, proportional to a^{-3}, whereas the volume elements producing the fields are proportional to a^3. Since the fields are proportional to $\chi\nu$, we can write $\omega(\mathbf{r}/a)=\frac{1}{3}\chi\nu\omega_v(\mathbf{r}/a)$, where $\omega_v(\mathbf{r}/a)$ is dimensionless and does not depend on χ, ν, D, or a. We will ignore (or separately take into account) relaxation in the bulk fluid and at surfaces. Since we are concerned only with transverse magnetization, and since we are not concerned with the uniform precession at the mean frequency, we may write the Bloch-Torrey equations for the magnetization M under the influence of diffusion, following Torrey [9], in complex form,

$$\frac{\partial M(\mathbf{r},t)}{\partial t}=iM(\mathbf{r},t)(\tfrac{1}{3}\chi\nu)\omega_v(\mathbf{r}/a)+\nabla\cdot D\nabla M(\mathbf{r},t)\ . \tag{1}$$

We now put this in dimensionless form by multiplying by the diffusion time a^2/D. We also express lengths (including in differential operators) in units of a and times in units of a^2/D. In the pore space D is assumed constant, and the subscripts u, v, or w will indicate the dimensionless variables throughout, giving

$$\frac{\partial M(\mathbf{r}_v,t_u)}{\partial t_u}=i(\tfrac{1}{3}\chi\nu)(a^2/D)M(\mathbf{r}_v,t_u)\omega_v(\mathbf{r}_v)+\nabla_u^2 M(\mathbf{r}_v,t_u)\ . \tag{2}$$

We see that the magnetization depends on $\mathbf{r}_u=\mathbf{r}_v=\mathbf{r}/a$ and $t_u=Dt/a^2$ and the dimensionless parameter

$\xi=\frac{1}{3}\chi\nu a^2/D$. In I it is shown that $\frac{1}{2}\chi\nu$ is roughly the maximum frequency deviation produced by the susceptibility difference χ. Thus, after precession for a time a^2/D, the maximum phase shift is about $3\pi\xi$. Note that χ and ν appear only as the product $\chi\nu$, and a and D appear only as the quotient a^2/D. We now integrate over the pore volume to see that the observed total magnetization (M in the following) is a function of only the two variables, ξ and t_u. We could, of course, use the variable $t_v=\xi t_u$ without introducing an additional degree of freedom. We can vary the parameters χ, ν, a, and D without changing $M(\tau_u)$ only as long as ξ is held constant.

B. Distributions of correlation times

In order to scale parameters without requiring that ξ be constant we must introduce some additional restriction, model, or assumption. We first turn to the model used in I and II, where we made the assumption that there was a substantial range of correlation times, τ_{ci} [defined following Eq. (4)] for change of precession frequency for spins diffusing through the variable local fields with local frequency variation ω. It was necessary to assume that the phase shifts at echo time for the various spins in the pore fluids are either small or else have a Gaussian distribution. We will in the present work conclude that the distributions are not Gaussian and, hence, that the first of these conditions is required. In I the correlation function F_{cc} is defined,

$$F_c(|t-t'|)=F_{cc}(t,t')=\int\int\omega(\mathbf{r}(t))\omega(\mathbf{r}(t'))dv\,dv' . \tag{3}$$

Thus F_c is determined completely by the probabilities of diffusing from the various initial positions to the various final positions in the time $t-t'$. These probabilities are governed by the diffusion equation, $\partial P/\partial t=\nabla\cdot D\nabla P$. We assume perfectly reflecting internal surfaces in the porous medium, although this is not strictly the case. We now rewrite (3) and the diffusion equation in dimensionless form, where, as before, the subscripts u, v, and w will be used to indicate the dimensionless variables. If D is constant in the pore space, the diffusion equation becomes simply

$$\frac{\partial P}{\partial t_u}=\nabla_u^2 P . \tag{4}$$

We now see that $F_c(|t_u-t_u'|)$ does not change its form with a linear scaling of the porous medium or with a change of the diffusion coefficient. As in I, F_c is resolved into a sum of exponential terms of the form $p_i\Omega_i^2\exp(-|t-t'|/\tau_{ci})$, where the p_i are signal fractions, and where Ω_i would be the rms value of ω if there were but a single correlation time.

Equation (23) of I gives the contribution of susceptibility differences χ to R for CPMG measurements, neglecting some small terms,

$$R\approx\sum_i p_i\Omega_i^2\tau_{ci}f(\tau/\tau_{ci}) ,\qquad f(x)=1-\frac{\tanh(x)}{x} . \tag{5}$$

We put this in dimensionless form by setting $\tau_{ciu}=D\tau_{ci}/a^2$, $\Omega_i=(\frac{1}{3}\chi\nu)\Omega_{iv}$, and $R_w=R_v/\xi=R_u/\xi^2$. We now have

$$R_w=\frac{RD}{(\frac{1}{3}\chi\nu a)^2}\approx\sum p_i\Omega_{iv}^2\tau_{ciu}f\left[\frac{\tau_u}{\tau_{ciu}}\right] . \tag{6}$$

The parameters p_i, Ω_{iv}, τ_{ciu} are now all properties of the *shape* of the porous medium and do not depend on χ, ν, D, or a. Thus, for a porous medium with a particular shape of pore space, R_w is the *same function* of τ_u, whatever changes are made in ξ, ν, D, or a. Equation (6) suggests that it should be possible to plot

$$R_w=\frac{RD}{(\frac{1}{3}\chi\nu a)^2}\quad\text{vs}\quad\frac{D\tau}{a^2}=\tau_u \tag{7}$$

in order to overlay $R(\tau)$ data taken with different values of ν, D, a, and χ within the range of applicability, $R\tau\ll 1$.

C. Slope of R vs τ

In I it was shown that, for CPMG measurements, a range of correlation times tends to give a substantial portion of the $R(\tau)$ curve that is nearly linear, making the slope of the nearly straight portion of the curve a useful parameter. It was shown that, for certain distributions of τ_{ci} values ranging over a decade or more, the extrapolated $\tau\to 0$ intercept of the nearly straight portion could, in principle, be either below or above the $\tau\to 0$ intercept of the complete function. In II it was shown experimentally that, for a sufficiently simple porous medium, $R(\tau)$ has zero initial slope and then has a substantial nearly linear portion before approaching a horizontal asymptote. If we define $\beta=\partial R/\partial\tau$, we have

$$\beta_v=\frac{\partial R_v}{\partial\tau_v}=\frac{1}{\xi^2}\frac{\partial R_u}{\partial\tau_u}=\frac{\beta}{(\frac{1}{3}\chi\nu)^2}=\frac{\partial R_w}{\partial\tau_u} . \tag{8}$$

From Eq. (6) we get

$$\beta_v=\sum_i p_i\Omega_{iv}^2 f'\left[\frac{\tau_u}{\tau_{ciu}}\right]=(\tfrac{1}{3}\chi\nu)^{-2}\frac{\partial R}{\partial\tau} . \tag{9}$$

where $f'(x)=df/dx$, and β_v depends only on the shape of the pore system. In Eqs. (8) and (9) we have defined a dimensionless slope that involves the susceptibility difference χ. However, in most NMR work in porous media we do not know χ, so we define a hybrid "practical" parameter β_ν, also dimensionless,

$$\beta_\nu=(10^{-6}\nu)^{-2}\frac{\partial R}{\partial\tau}=(\tfrac{1}{3}\times 10^6\chi)^2\beta_v . \tag{10}$$

In ranges of the parameters where it can be measured, the dimensionless slope, whether expressed as β_v or β_ν, is notably independent of ν, D, and a. As can be seen from Eq. (9), substituting a liquid with different D, or changing temperature to change D, should not greatly affect the slope of the nearly linear portion of $R_w(\tau_u)$ or of $R(\tau)$. If any part of the porous system is paramagnetic or ferromagnetic, a temperature change might, however, affect

ξ. Note that the relaxation rates of the bulk fluids and the surface contributions to relaxation may change with temperature; however, R is the *incremental* rate due to diffusion in the local fields due to susceptibility differences. If it is experimentally possible to scale the dimensions of the porous medium without changing the shape of the pore system, this too should not change the slope of the nearly linear portion of $R(\tau)$ or $R_w(\tau_u)$.

The maximum value of the function f' is computed from Eq. (5) to be about 0.34; however, an assumed distribution of correlation times ranging over a factor of 20 gives a substantial section with a slope of $\sum p_i f_i' = \langle f' \rangle = 0.19 \pm 0.04$, where $f_i' = f'(\tau/\tau_{ci})$, with the τ's in any consistent units. We can now use 0.19 for f' in Eq. (9) to relate the slope of the nearly linear portion of $R_w(\tau_u)$ to measured values of β_v if we have a simple porous medium with a relatively narrow range of τ_{ciu} values. The value of $\langle f' \rangle$ should be smaller, but the nearly linear range longer, if there is a wide range of τ_{ciu} values. We now make the approximation

$$\beta_v = \sum_i p_i \Omega_{iv}^2 f_i' \approx \langle \omega_v^2 \rangle \langle f' \rangle \approx 0.19 \langle \omega_v^2 \rangle \ . \tag{11}$$

We can use the measured value $\beta_v = 1.32$ to be discussed in Sec. IV to get from Eq. (11) an estimate, $\langle \omega_v^2 \rangle \approx 6.9$.

D. Tentative Cauchy distribution of phases

In I it is shown that, for practical purposes, the field variations due to susceptibility differences are limited to about $\pm\frac{1}{2}\chi B_0$, where B_0 is the static field of the NMR instrument. Correspondingly, the variation ω of the local angular frequency from the mean angular frequency ω_0 is limited to $\pm\frac{1}{2}\chi\omega_0 = \pm\pi\chi\nu$. Within these limits on ω the actual distribution in ω depends on the nature of the porous medium. The data to be presented here are for porous media with relatively high porosity and with relatively simple and uniform pore structures. As mentioned in I, if much of the fluid is in well defined pores, as opposed to crevices and channels, there is likely to be a substantial volume near the centers of pores, where the field is nearly uniform, with $\omega \approx 0$. In the extreme case of an isolated spherical or elliptical pore the field is uniform, but for the samples considered here the pores are very well connected and therefore not isolated. Thus we may assume that ω is very small for at least half of the pore space (near centers of pores) and that the distribution for the rest tapers to 0 at $\omega = \pm\pi\chi\nu$. This distribution would have a central peak narrow compared to $\pi\chi\nu$ and have extensive tails. As discussed at length in I, Eqs. (5)–(9) require that phase shifts accumulated between echoes (for CPMG, or at echo time for single echoes) by spins in various parts of the pore space either be comparable to or less than unity or else have a Gaussian distribution. The above intuitive distribution of ω is clearly not Gaussian. Furthermore, it will be seen that the asymptotic values of R from CPMG data are *not* proportional to $\tau_{ci} \propto a^2/D$ and *not* proportional to $\Omega_i^2 \propto \chi^2\nu^2$, as required by Eq. (5).

We can get information on the asymptotic values of R from the CPMG data themselves if they can be carried out to sufficiently large τ values, as in I. However, we can better infer the CPMG asymptotic values from Hahn single-echo T_2 data. The logarithm of the echo amplitude as a function of echo time $t = 2\tau$ starts with zero slope (neglecting decay from sources other than diffusion through local fields) and approaches a region of nearly constant slope $-R_s$ after a time of the order of $t = 1/R_s$, if this provides sufficient time for diffusion that refocusing is not very efficient by echo time. This last condition will be found empirically to be roughly equivalent to $\xi < 2$ for the present measurements and with the present definition of a. The asymptotic rate for the CPMG measurements and R_s should be equal. The refocusing pulses cancel effects of fields that are inhomogeneous over longer distances than spins can diffuse in measurement times, but they are not effective at canceling phase shifts due to diffusion in the local field ω and accumulated at times sufficiently far away from refocusing pulses. The single-echo measurements at a given τ value have the decay reduced by the refocusing. The approximately straight part of the $-\ln M$ curve is raised a fixed amount by the refocusing if the effect of the refocusing is roughly to cancel decay for a certain length of time. Thus the slope gives the rate in the *absence* of refocusing of the effects of the grain-scale local field ω but *with* refocusing of the effects of the larger-scale fields. Since the asymptotic rate for CPMG measurements of $R(\tau)$ is also the rate in the absence of refocusing of the effects of the grain-scale local fields, the slope of the single-echo curve gives the asymptotic rate of the CPMG curve for $R(\tau)$, and it can be determined reliably at much shorter times.

For the present measurements these asymptotic rates, inferred from the single-echo data, are proportional to the *first* power of ν rather than the square, and they still do not depend on a or D. This is compatible with the above surmise that the distribution of ω may have a substantial tail and suggests that the distribution of ω might approximate a Cauchy distribution, $[(\omega/R_s)^2+1)]^{-1}/(\pi R_s)$, where R_s is the half-width and which has statistical properties very different from those of a Gaussian. Brown [6] has shown that this is the distribution that would result from randomly placed dipole sources and that it leads to the free induction decay $\exp(-R_s t)$. Furthermore, it was made plausible by theory and confirmed by experiment that diffusion does not affect the rate. That is, motional line narrowing is suppressed, because the distribution with the long tail leads to some large phase shifts owing to diffusion, offsetting the effects of averaging. Once again, the decay is reduced for some time in the vicinity of the refocusing pulses, but the incremental decay with increase of τ is, at long-τ values, the same as for free precession ("corrected" for larger-scale field variations), and (for an ideal Cauchy distribution of phases) it is independent of a^2/D if the echo time is substantially larger than a^2/D.

In Sec. IV it will be seen that, if $\xi < 2$, $R_s = (\frac{1}{3}\chi\nu)R_{sv}$, where $R_{sv} \approx 1$ for the present measurements and depends only on the shape of the pore space. This is equivalent to $R_{su} = R_s(a^2/D) = R_{sv}\xi \approx \xi$. Thus $R_s t = R_{su} t_u \approx \xi t_u$ for our data. In time a^2/D the decay is by about ξ Np (nepers, factors of e). The maximum value of $|\omega|$, ap-

proximately $\pi\chi v$, is $9.4R_s$. To use these values to get another estimate of $\langle\omega_v^2\rangle$, we compute $\langle\omega_v^2\rangle = \int_0^{9.4}[x^2/(x^2+1)]dx / \int_0^{9.4}[1/(x^2+1)]dx = 5.4$ for the Cauchy distribution truncated at the maximum $|\omega|$. The two values of $\langle\omega_v^2\rangle$, 6.9 and 5.4 are close to each other, even though one comes from data for the short-τ regime, where R is proportional to $(\frac{1}{3}\chi v)^2$, and the other from data for the long-τ regime, where R is proportional to $\frac{1}{3}\chi v$. In the small-τ region, where $|\varphi|_{\max} \lesssim 1$, only $\langle\varphi^2\rangle$ is significant in determining echo decay; the shape of the distribution does not matter. However, assuming the truncated Cauchy distribution also at small τ gives roughly the right width of the Cauchy distribution for use at larger τ.

The free induction decay (FID) at time t due to a Cauchy distribution of angular frequencies with half-width R_s and without diffusion is a simple exponential decay, $\exp(-R_s t)$. The effects of diffusion are not easy to account for in precise detail for an actual porous medium, but it is instructive to consider the consequences of the instantaneous random relocation (nonphysical) of all spins at intervals of a time τ_e (e for exchange). Of course, the results of the actual diffusion are more complicated than a periodic complete exchange, and, in particular, the spins away from the centers of the larger pores probably change fields more quickly that those near the centers. The distribution of the results of $n = t/\tau_e$ random choices from any distribution is an n-fold convolution of the distribution. The Fourier transform (FT) of the n-fold convolution is the nth power of the FT of the original distribution. The logarithm of the resultant FT is n times that of the original FT. Thus, for an untruncated Cauchy distribution without exchange, the natural logarithm of the FT would be $-R_s t$. With exchange, we would have $(-R_s\tau_e)(t/\tau_e) = -R_s t$. That is, the exchange has no effect. We do not get the "averaging" effect we would get with a Gaussian distribution.

If diffusion is fast enough that the missing part of the tail of the truncated Cauchy distribution of phases would have been sampled by most spins, including those near centers of pores, then R_s will be somewhat less than computed from the full Cauchy distribution. As seen above, the distribution is truncated at $x_0 \approx 9.4$ times its half-width. The normalized distribution is $g(x) = (2\tan^{-1}x_0)^{-1}(x^2+1)^{-1}$ for $|x| < x_0$, and zero elsewhere. The FT $G(y)$ is given by a series expansion, which is convenient for computation,

$$G(y) = \sum_{k=0}^{\infty} \frac{y^{2k}}{(2k)!}\left[1 + \frac{1}{\tan^{-1}x_0}\sum_{r=1}^{k}(-1)^r\frac{x_0^{2r-1}}{(2r-1)}\right]. \tag{12}$$

A semiconvergent series can be used for $y(x_0^2+1) \gg 1$,

$$G(y) \approx e^{-y} + \frac{\sin(x_0 y)}{y(x_0^2+1)} - \frac{2\cos(x_0 y)}{y^2(x_0^2+1)^2} + \cdots . \tag{13}$$

The natural logarithm of the FT starts with zero slope and then oscillates gently about the line $-(y-y_0)$, where $y_0 = \ln[\pi/(2\tan^{-1}x_0)]$. For $x_0 = 9.4$, we have $y_0 = 0.070$. Repeated sampling would still give straight-line decay of the natural logarithm of the FID, but the truncation of the phase distribution at x_0 would reduce the slope by the ratio $G(y_e)/G_0(y_e)$, where $G_0(y) = e^{-y}$ is the untruncated FT and $y_e = R_s\tau_e \approx R_{sv}\xi\tau_{eu}$ (with $R_{sv} \approx 1$ for our particular data set). This ratio starts at zero and eventually approaches 1.0. It reaches 90% at $y = 0.5$. To have decay of single-echo curves with at least 90% of the maximum rate, we need (for our data set) $\xi\tau_{eu} \geq 0.5$.

The smallest ξ for our set of data is 0.031. To have $\xi\tau_{eu} \geq 0.5$ requires $t_{eu} \geq 16$; that is, the exchange time must be 16 times the nominal diffusion time a^2/D. This at first seemed unlikely, but we note that a is an effective pore entrance radius (see Sec. III), probably smaller than a pore radius. (It is not intended to imply that the pores are spherical or that they are connected by cylinders.) Furthermore, as discussed in I, diffusion over distances of the order of a pore *spacing* would be required for many spins to reach regions of highest or lowest fields, with the times required going as the squares of the distances. A further factor leading to long τ_e's is that diffusion is restricted by barriers. The exchange times may be longer than the longest significant correlation times, because spins in pores, as opposed to channels and spaces between pores, probably do not have to diffuse as far to lose correlation as they do to have the appropriate probability of visiting a region of highest $|\omega|$.

E. Arctangent fits to the data

In I it was shown that wide distributions of correlation times led to $R(\tau)$ that was well approximated by an arctangent function. In II it was shown that moderately narrow distributions could be fit by adding an exponential buildup term with time constant T_4. Here, instead of the exponential term, we will use another arctangent factor, giving much the same effect.

$$R \approx R_s\left[\frac{2}{\pi}\tan^{-1}\left[\frac{\pi}{2}\tau/T_3\right]\right]\left[\frac{2}{\pi}\tan^{-1}\left[\frac{2}{\pi}\frac{\tau}{T_4}\right]\right]. \tag{14}$$

The expressions in square brackets are normalized to range from zero to one, with the term in the first set of brackets giving the initial slope τ/T_3. The initial τ dependence is quadratic, as required by Eq. (5). The term in the second set of brackets gives a delay of T_4 if we have $T_4 \ll \tau \ll T_3$:

$$R \approx R_s[\tau/T_3]\left[\frac{2}{\pi}\left[\frac{\pi}{2} - \frac{\pi}{2}\frac{T_4}{\tau}\right]\right]$$
$$\approx R_s(\tau - T_4)/T_3 = \beta(\tau - T_4), \tag{15}$$

which represents the approximately straight-line portion of the curve, where the slope is $\beta = \partial R/\partial\tau = R_s/T_3$.

Equations (14) and (15) can be put in dimensionless form by multiplying by the diffusion time a^2/D; the subscript u can simply be added to each symbol. However, as has already been noted, $R_{su} = \xi R_{sv}$. Equation (8) shows that the slope of the linear portion (when there is one), $\partial R_u/\partial\tau_u = R_{su}/T_{3u} = \xi^2\beta_v$, giving $T_{3u} = R_{sv}/(\xi\beta_v)$.

We use $\tau_u = D\tau/a^2$ and $T_{4u} = DT_4/a^2$, leaving $\tau/T_4 = \tau_u/T_{4u}$. The parameters T_{4u}, R_{sv}, and β_v should depend only on the *shape* of the porous medium. Equation (14) now becomes

$$R_w \approx \left[2\frac{R_{sv}}{\pi\xi} \tan^{-1}\left[\frac{\pi\xi}{2R_{sv}} \beta_v \tau_u \right] \right] \times \left[\frac{2}{\pi} \tan^{-1}\left[\frac{2}{\pi} \frac{\tau_u}{T_{4u}} \right] \right] . \quad (16)$$

If $\xi\beta_v\tau_u/R_{sv} \ll 1$, the factors $2R_{sv}/(\pi\xi)$ cancel, and Eq. (16) becomes

$$R_w \approx \beta_v \tau_u \left[\frac{2}{\pi} \tan^{-1}\left[\frac{2}{\pi} \frac{\tau_u}{T_{4u}} \right] \right] . \quad (17)$$

This is the regime for which experimental points for different parameter values should overlie when plotted according to Eq. (7). The overlay will not continue beyond $\xi\beta_v\tau_u/R_{sv} \ll 1$, because ξ then becomes a parameter in Eq. (16). Equation (7) then ceases to apply because of not meeting the requirement given in I of having, at echo time, either a Gaussian distribution of phases or else all phases $\lesssim 1$. We now believe, as we have discussed above, that for most parameter regimes the Gaussian condition is not even approximated; the second condition is essentially $R\tau \ll 1$. That is, there should be several CPMG echoes in a relaxation time.

We have discussed single echoes for longer echo times and for greater decay, although with the limitation that $\xi < 2$ (with a defined as for our data). We are interested also in echo amplitudes for $\xi \gtrsim 2$, especially for single spin echoes, where we can follow the decay for one or two decades per echo. We have tried using the equivalent of Eq. (6) to compute $\langle \varphi^2 \rangle$ beyond the range where $R\tau \ll 1$ and then using the rms phase and assuming a Cauchy distribution. However, this appears to be taking the combination of the model of I and the assumed Cauchy distribution of phases too literally; the results do not adequately fit our data.

For a value of t_v in the range of moderate decay, which is $1 < t_v < 6$ for $\xi < 2$ (for our data set), we note that increasing ξ at a fixed t_v gives decreasing $t_u = t_v/\xi$. This eventually leads to slower decay both because of more complete refocusing of individual spins and because of increased isolation of spins in regions of lowest field gradients. For large ξ and single spin echoes in porous media we can expect a situation partially analogous to the diffusion-limited surface effect, where relaxation is determined by diffusion independently of the strength of the surface effect so long as it is above some threshold. Since $t_v = \xi t_u$, we can phase out a factor of ξ (containing the dephasing rate $\frac{1}{3}\chi v$) as ξt_v becomes large by again using the arctangent function as a phase-out function and multiply the $\ln M(t_v)$ by the factor

$$\frac{\tan^{-1}\sqrt{\tau_w/T_{5w}}}{\sqrt{\tau_w/T_{5w}}} . \quad (18)$$

By our convention $\tau_w = \xi\tau_v = \xi t_v/2 = \xi^2 t_u/2$, and T_{5w} appears to depend on shape only. The factor Eq. (18) ≈ 1 if $\xi t_v/(2T_{5w}) \ll 1$. We saw that for $\xi < 2$, $-\ln M = R_{sv} t_v \approx t_v$ minus a small delay. Multiplying this by Eq. (18) gives $\ln M \propto \sqrt{t_u}$ for large ξt_v. Although this limit does not explicitly involve χv, it does indirectly, since we have required that t_v be in the range for substantial decay.

The asymptotic $-\ln M$ for a compact single pore or periodic pore system is not proportional to $\sqrt{t_u}$, but simply proportional to t_u. However, there is usually some range of pore sizes and significant variation in the channels between pores. The decay factor $\exp(-\sqrt{t_u})$ is the Laplace transform of $r^{-3/2}\exp[-1/(4r)]$, which is the distribution of rates for $\exp(-\sqrt{t_u})$. If we convert to a time $x = 1/r$, with $dr = -dx/x^2$, we get a distribution proportional to $(1/\sqrt{x})\exp(-x/4)$. We are not concerned with this distribution at short times, because $-\ln M$ is not proportional to $-\sqrt{t_u}$ at short times. We note that this distribution does not extend to implausibly long times. In any case, Eq. (18) is a largely empirical expression that accounts well for the effects of moderately large ξ for our data.

III. EXPERIMENT

The samples used in this work are microporous porcelain samples (Selas Floctronics) with exceptionally smooth pore surfaces, made with controlled pore sizes for use as filter materials. The A samples have pore entrance radii $a \approx 0.6$ μm and the B samples $a \approx 1.5$ μm, determined from capillary pressures by the injection of mercury. Porosities are about 0.30 and 0.50, respectively. The volume magnetic susceptibilities of the solid framework materials (not of the macroscopic porous solid) are $\chi_A \approx +48.62\times10^{-6}$ and $\chi_B \approx +45.48\times10^{-6}$. These are in Système International (SI) units, dimensionless, but 4π times their values in the emu or Gaussian units often used in tables. These materials are described in more detail elsewhere [27]. It was necessary to use physically different samples of the solid materials for the different saturating fluids and for the two different NMR instruments to be mentioned. Although the materials are exceptionally uniform, some variation is inevitable, and it necessarily induces some scatter in comparisons of scaled data.

The saturating liquids used were brine [27] and two oils, Soltrol-130 [27] and Soltrol-170, made by Philips Petroleum Co. The diffusion coefficients in $(\mu m)^2$/ms at 25 °C are 2.14, 0.728, and 0.401, respectively. At 41 °C they are 3.178, 0.965, and 0.571. The volume magnetic susceptibility, in SI units, of the brine is $\chi_W = -9.062\times10^{-6}$, and that of both oils is $\chi_S = -8.225\times10^{-6}$. For brine in A, $10^6\chi = 48.623 - (-9.062) = 57.7$. For B, $10^6\chi = 54.5$, about 6% less than for A. For either Soltrol χ is about 1.5% less than for the brine. Although χ^2 is about 12% higher for A than for B, the β_v values [see Eq. (10)] and also the R_{sv} values (see Fig. 1) are the same for A and B within experimental accuracy. We have therefore used the value of χ_B for both porous materials in order to overlay data points. We do not regard 12% as a significant discrepancy, since

the porosities of the two materials are significantly different, indicating that the internal geometries are not simply linearly scaled from one to the other. The 1.5% smaller χ for the oil-saturated samples than for the brine was still taken into account.

CPMG and single-echo measurements were made at 41 °C with brine in B and with Soltrol-130 in B at $\nu=20$ MHz with a modified Bruker Minispec instrument [27], which had the advantages of a relatively short (5 μs) 90° pulse width and which permitted recording 2048 echoes in a CPMG sequence, thus allowing about 300 ms of data even when $\tau=75$ μs (150 μs echo spacing). For this measurement only, the internal surfaces of the porous medium were coated with a water repellent material [27] in an attempt to minimize any tendency of the fluid molecules, particularly water molecules, to stick to the pore surfaces. The coating did not, however, greatly affect either longitudinal or transverse relaxation times. The Minispec measurements were made a year earlier than the others, and the samples were from a different batch of the porcelain.

CPMG measurements at 25 °C using a variable-frequency instrument [28] were made, using phase cycling, at 10, 20, and 50 MHz, with all combinations of the two porous solids and three fluids. The 90° pulse widths at these frequencies were 14, 20, and 23 μs, respectively. Only 512 echoes could be recorded, limiting the length of the recorded echo train to about 50 ms for $\tau=50$ μs.

Longitudinal relaxation curves were run for all combinations of solids, liquids, and frequencies; relaxation was substantially single exponential in all sample combinations and for both instruments. The stretched-exponential α factor was 0.993 ± 0.003.

As discussed in I and II, some special procedures are needed in interpreting CPMG data as a function of τ when relaxation is not a single-exponential decay. When there is substantial relaxation by the time of the first data point, there is no direct way to get information on exponential components with shorter times. We address this problem by adding a virtual zeroth echo to each data set. The echo No. 0 comes from extrapolation of the echo trains with the several shortest τ's, which for the present data give very close to the same values. For a sample with a narrow distribution of correlation times and for τ of the order of the correlation times it can be seen from Eq. (19) of I that a small but non-negligible error is made by dropping a small term that is not proportional to echo time. This error is, however, *far* smaller than that using the CPMG data without the virtual zeroth echo.

The relaxation data for the CPMG measurements were fit by discrete sums of exponentials. In each case about 90% or more of the signal amplitude had T_2 values within a range of a factor of about 3 if the components contributing more than a few percent of the signal were covered by the data for the particular τ value. As mentioned, for the shortest τ's the longest relaxation times could not be covered, and coverage shorter than 2τ is inherently unavailable for the long τ's. The relatively narrow distributions of T_2's confirm the relative uniformity of the solid samples. The distributions of times tend to be widest for smallest D, largest a, and largest ν. This is as expected, since short diffusion lengths, short relaxation times, and large pore spacings give the opportunity for spins to sample more isolated portions of the pore space. It is the relative uniformity of the pore space in the present samples that gives the opportunity to illustrate at least roughly the effects of ν, D, a, and χ.

We have taken for the relaxation time the time for decay by a factor of $1/e$, using multicomponent exponential fits for interpolation. This appears to give the most robust T_2 values available with the present experimental conditions and objectives. We have avoided using T_2 values comparable to or shorter than the first data time or significantly longer than the longest data time.

Some of the T_2's are considerably longer than the data recording time for the variable-frequency spectrometer when the shortest τ's are used. Especially for the variable-frequency spectrometer, the 90° pulses are too long to be neglected, or to permit reliable correction of the T_2 data, for the shortest τ's (50 μs). We have made a correction assuming phase locking during the pulses, with relaxation at the rate $1/T_{1\rho}=1/T_2(\tau\rightarrow 0)$. This presents obvious difficulties when R is large even for small τ's. Thus, although data were taken for τ from 50 μs to either 2.0 or 2.4 ms, some of these points must be omitted from the data sets for the above reasons.

For all but sample A with brine the portion of the $R(\tau)$ curve at small τ preceding the roughly linear portion is at least partly within the range of measurements. A nonlinear search was used to correct the data for the 90° pulse width and, at the same time, to fit the corrected $1/T_2$ as a function of τ to the form shown in Eq. (16) for the Minispec data and Eq. (17) for the rest of the present work, where the data were not carried out beyond the nearly linear portion of the curve.

IV. RESULTS AND DISCUSSION

Figure 1(a) shows the single-echo decay curves from the variable-frequency instrument at 25 °C, with $\ln M$, the natural logarithm of echo amplitude, plotted against the dimensionless echo time $t_v=\frac{1}{3}\chi\nu t$. The sets of points are

TABLE I. Diffusion time, dephasing rate, and ξ. The last three column headings show the measurement frequency ν above the dephasing rate $\frac{1}{3}\chi\nu$. The rows show sample identification (1 for brine, 2 for Soltrol-130, 3 for Soltrol-170) followed by the diffusion time a^2/D. The remaining table entries are $\xi=\frac{1}{3}\chi\nu a^2/D$, which is the product of diffusion time and dephasing rate.

Sample	a^2/D (ms)	10 MHz 0.182/ms	20 MHz 0.363/ms	50 MHz 0.908/ms
A1	0.168	0.031	0.061	0.153
A2	0.495	0.090	0.180	0.449
A3	0.898	0.163	0.326	0.815
B1	1.051	0.191	0.382	0.995
B2	3.091	0.561	1.123	2.807
B3	5.611	1.019	2.039	5.097

arranged in the order of increasing ξ, starting from the bottom, with the specific order shown in the figure caption and the ξ values shown in Table I. With the exception of the top few sets of points, those with $\xi \gtrsim 2$, the straight-line portions of the ln$M$ curves all have slopes of approximately -1, corresponding to $R_{sv} \approx 1$. The numerical value of this slope, of course, depends on the choice of coefficient in defining the dephasing rate $\frac{1}{3}\chi v$ used in defining t_v. However, the fact that there are substantial sections of the ln$M$ curves that are approximately straight and that the slopes are roughly equal for a wide range of values of a, D, and v support the hypothesis, presented in Sec. II D that the distribution of phases at echo time is approximately a Cauchy distribution rather than a Gaussian.

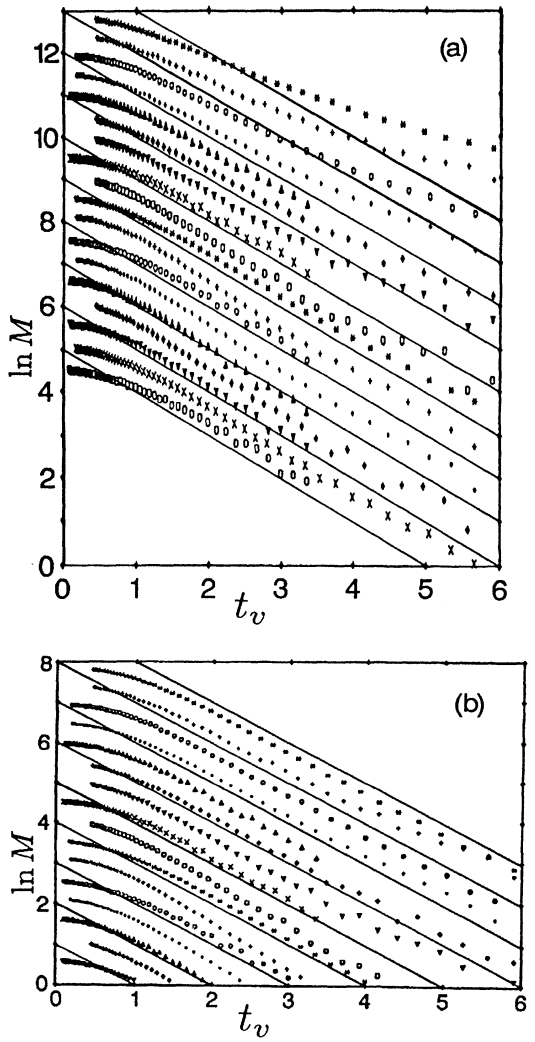

FIG. 1. Single-spin-echo points, with ln$M$, the natural logarithm of echo amplitude in nepers, plotted against $t_v = \frac{1}{3}\chi v t$ (dimensionless), where $t = 2\tau$ = echo time. The curves are shifted vertically for display. The curves are, from bottom to top, shown in increasing order of $\xi = \frac{1}{3}\chi v a^2/D$, ranging from 0.03 to 5.1. Individual ξ values are given in Table I. The sample-combination sequence is A11, A12, A21, A15, A31, A22, B11, A32, B12, A25, B21, A35, B15, B31, B22, B32, B25, B35, where A indicates the porcelain material with measured pore entrance radii $a = 0.6$ μm and B with $a = 1.5$ μm. The middle symbol is 1 for brine ($D = 2.14$ μm^2/ms), 2 for Soltrol-130 ($D = 0.728$), and 3 for Soltrol-170 ($D = 0.401$). The last symbol is the frequency in MHz divided by ten. (a) shows all 18 data sets as measured. Note that, except for the top three to six sets of points, those with $\xi \gtrsim 2$, the asymptotic slopes $-R_{sv}$ are close to -1. (b) all displayed points for the data sets with largest ξ values are divided by the functions in Eq. (18) to compensate for the effects of large ξ, using $T_{5w} = 5.0$.

Figure 1(a) shows ln$M$ values just as they are measured, except with vertical shifts for display convenience. The diagonal lines with slope -1 are for comparison with the sets of points. Note that the sets of points approach asymptotes parallel to the diagonal lines except for the top few, those with $\xi \gtrsim 2$. Here, the slopes are significantly less than for smaller ξ, and furthermore, there is a tendency for the slope to decrease after a region of maximum slope. For instance, for the top curve (B35) the slope is about twice as great at $t_v = 2.3$ as it is at 6.0. This is expected, since much slower diffusion leads to smaller frequency changes during diffusion and to more complete refocusing. Spins that start near centers of larger pores may be efficiently refocused before diffusing to regions of more inhomogeneous fields. At the other extreme is sample A11, $\xi = 0.031$, which has about the same slope as the rest of the curves. As mentioned in Sec. II D, we must assume that exchange times due to diffusion are at least $16a^2/D$. There does not yet appear to be significant motional narrowing, but still smaller ξ values would presumably lead to longer decay times than would be computed from the untruncated Cauchy distribution.

Figure 1(b) shows the points, with ln$M$ divided by the "correction" factor Eq. (18), attempting to compensate for the effects of the larger ξ's. Note that all sets of points now approach approximately the same slope. The effectiveness of this compensation suggests the plausibility of phasing out a factor of ξ as ξt_v increases. It would be better tested if our data went to larger ξ.

In Figs. 1(a) and 1(b) it can be seen that ln$M$ at echo time is roughly quadratic in t_v for $t_v < 1$. The decay by $t_v = 1$ is a little less than 0.5, and the straight-line portion extrapolates to a little more than 0.5 Np above the value for $\tau \rightarrow 0$. Actually, as can be seen from Eqs. (16) and (17), the initial dependence is cubic for a short time $t_v = 2\tau_v = 2T_{4v} = 2\xi T_{4u}$, where $T_{4u} \approx 0.06$ for our data.

Parameters from CPMG measurements, such as T_{4u} and β_v, should apply roughly to the single-spin-echo curves when the distribution of CPMG relaxation times is fairly narrow, as it is here.

For those of our data which are in the range for Eq. (15), which includes some points for all sets but those with the largest ξ's, we can see from Eq. (15) that, with the assumption of small phase shifts for the first echo, $-\ln M \approx 0.5$ is about the amount of decay where the assumption of small phase shifts ceases to be valid and starts to lead to an overestimate of the decay if the phases have a Cauchy distribution. For $T_4 \ll \tau \ll T_3$, Eq. (15) gives us, after some manipulation of units, $-\ln M = \frac{1}{2}\langle \varphi^2 \rangle = \frac{1}{2}\beta_v t_v (t_v - 2\xi T_{4u}) \approx \frac{1}{2}\beta_v (t_v - \xi T_{4u})^2$. For de-

cay by 0.5 Np we have $t_v=\beta_v^{-1/2}+\xi T_{4u}$, with $\beta_v=1.32$ and $T_{4u}=0.06$ for the present data. The actual time would be slightly longer because of the long-tailed distribution of phases "wasting" a small portion of its computed $\langle\varphi^2\rangle$ on "overkill." In any case the agreement with the behavior in Fig. 1 is good.

We get $\beta_v\approx 435$ from CPMG data at 25 °C for all combinations of sample, fluid, and frequency for which β_v can be measured by the variable-frequency instrument. In Eq. (7) D/a^2 ranges over a factor of about 33, so that for Soltrol-170 in B one may expect not even to reach the linear portion of $R(\tau)$, making it difficult to estimate β_v. For these reasons the best measurements of β_v can be expected for the largest D with the smallest a and ν, that is, for brine in sample A at 10 MHz. Good measurements of β_v were obtained, all within 2% of the above value, for brine in A at 10 MHz and at 20 MHz, for Soltrol-130 in A at 10 MHz, and for brine in B at 10 MHz. The remaining measurements do not cover the nearly linear portion of $R(\tau)$ as well as these do; however, values within about 10% were obtainable for all A combinations except with Soltrol-170 at 50 MHz and for B only with brine at 10 and 20 MHz and (marginally) with Soltrol-130 at 10 MHz. As can be seen from Table I, these correspond to the combinations for which $\xi<0.7$.

For the earlier Minispec measurements at 41 °C on the sample which had been made water repellent and which came from a different batch of the material, β_v was about 18% less. The material is paramagnetic, but the temperature difference would appear to account for only half of the 18% if magnetization is proportional to K^{-1}.

Figure 2 shows plots scaled as indicated in Eq. (7) for brine in sample B and for Soltrol-130 in B at 41 °C. These Minispec data provide adequate coverage for short τ values. The D ratio of the two fluids is 3.29, so the brine point for $\tau=75$ μs is midway between the Soltrol-130 points for 200 and 300 μs. The two curves agree in both amplitude and slope over the short region of overlap. The two data sets are processed independently without any inference of parameters from either for the other. The solid curves, however, are derived from the same values, $R_{sv}=0.845$ (from single-echo data), $\beta_v=1.096$ (from CPMG data), and $T_{3v}=R_{sv}/\beta_v=0.77$, together with their individual values of ξ. The scaling rule of Eq. (7) appears to fit precisely for the range where $\tau/T_3=\xi\tau_u/T_{v3}\ll 1$. The complete fit, Eq. (16), is very good for the brine-saturated sample, for which $\xi=0.257$ (not in Table I, which is for 25 °C). The fit is less good, but not wild, for the last two points for Soltrol-130, with $\xi=0.847$. Not surprisingly, a better fit can be made individually, without reference to R_s from single-echo data and without imposing exactly the same β_v on both cures. In this case the values of T_3 increase slightly with increasing a^2/D.

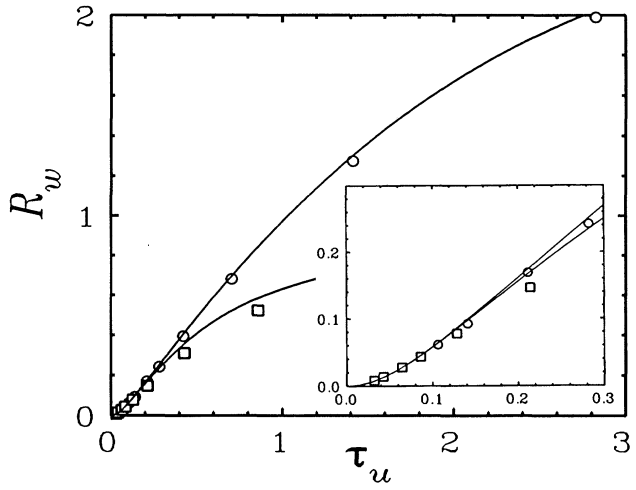

FIG. 2. CPMG data for porcelain B treated for water repellency and saturated separately with brine and with Soltrol-130 at 41 °C. The ordinate is $R_w=RD/(\frac{1}{3}\chi\nu a)^2$ (dimensionless), and the abscissa is $\tau_u=D\tau/a^2$ (dimensionless). The two data sets are fit by Eq. (16) with $R_{sv}=0.845$, $\beta_v=1.096$, $R_{3v}=\beta_v/R_{sv}$, and $T_{4u}=0.06$. For the upper curve (brine, circles) $\xi=0.257$ and for the lower curve (Soltrol-130, squares) $\xi=0.847$. The value of R_{sv} is derived form the slope of the single-echo data (not shown for these two samples). The small-t_v region is expanded in the inset.

Data from the variable-frequency instrument are shown in Fig. 3 with all valid points for all combinations of porous samples, liquids, and frequencies. The range of

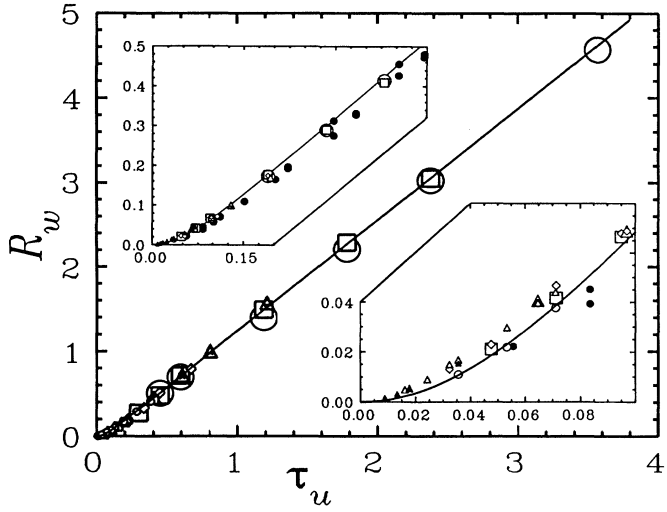

FIG. 3. CPMG data (ordinate and abscissa as in Fig. 2) up to and including the nearly straight portions of the curves for 25 °C for all combinations of solid material, saturating fluid, and frequency. In the central plot symbol size decreases with increasing ξ down to a minimum size. The large circles are for A11, the large squares for A12, the large triangles for A21, and the diamonds for A15. The solid curve is Eq. (17), with $\beta_v=1.32$ and $T_{4u}=0.06$. The scale of the upper inset is expanded to show both A and B points for intermediate τ_u, with A points shown as solid circles. Large circles are B11, large squares B12, triangles B21, and diamonds B15. The lower inset is further expanded to show the transition region between quadratic and linear dependence of R_w on τ_u, again with the A points shown as solid circles. The small solid triangles are B35, the small open triangles B25, the small diamonds B32, and the small circles B22. The large triangles are B31, and the large squares are B12.

τ_u is over a factor of 400, so only a small fraction of the points can be shown clearly in one plot. As can be seen from the central plot in Fig. 3, $R_w(\tau_u)$ is roughly linear over a factor of about 40. All of the points with $\tau_u > 0.6$ are for sample A. To minimize the problem of plotted symbols hiding each other, the symbols decrease in size, down to a minimum, as ξ increases. The upper inset in Fig. 3 shows the range covered by points from both A and B, with the A points all shown as filled circles. The plot of the dimensionless parameters, scaled for substantial ranges of D, a, and ν, forms a single smooth curve within the accuracy of the measurements. The lower inset in Fig. 3 shows a still more expanded plot, with the same symbols as in the upper inset. There is still good overlay of the scaled points. There is some scatter, and the A points tend to be slightly below the B points. However, as mentioned, there is some uncertainty in the extrapolation of $R_w(\tau_u)$ for $\tau_u \to 0$, and the pore structure of B is not a simple linear mapping of that of A.

V. SUMMARY

CPMG and single-spin-echo data have been taken over substantial ranges of ν, a, and D. The results are compatible with the general feature of the model of I and II, which predicts that R_w is a function of τ_u if $R\tau \ll 1$. The results are also compatible with the more specific feature, where a distribution of correlation times leads to a substantial nearly linear portion of $R_w(\tau_u)$ or $R(\tau)$. Limitations of the model for $R\tau \ll 1$ are discussed in I and II. In more complex porous media CPMG relaxation times may span several decades, however short τ may be. It was shown in II that for a porous sandstone the τ dependence of R was very different for the long relaxation time components than for the short ones. Any scaling of parameters must be considered separately for different parts of the relaxation time spectrum. It is to make more interpretable comparisons of single-echo and CPMG measurements that we have chosen the porous porcelains, with their relatively uniform pore structure and relatively narrow spectra of T_1 and T_2.

For a relatively homogeneous porous medium with a narrow distribution of transverse relaxation times the single-echo $\ln M$ curve approaches a nearly constant asymptotic slope $-R_s$ if $\xi < 2$, and R_s is also the asymptotic value of $R(\tau)$ for CPMG measurements. For this asymptotic region, R_u $(=\xi^2 R_w)$ is found to be proportional to ξ rather than to ξ^2, as would be predicted by the model of I. As discussed in Sec. II D, assumption of a truncated Cauchy distribution of phases would give the observed first-power dependence on ξ, and the second moment of the truncated Cauchy distribution derived from single-echo data at $t_v = 2\tau_v \gg 1$ is compatible with that derived from CPMG data at $\tau_v \ll 1$. The observed lack of dependence of R_{sv} on a^2/D is also compatible with this assumption.

The slope of the nearly linear part of $R(\tau)$ for the CPMG data is independent of a and D for $R\tau \ll 1$. The asymptotic value of $R(\tau)$ is also independent of a and D if $\xi < 2$. Equation (16) appears to represent $R_w(\tau_u)$ adequately for any value of τ_u if $\xi < 2$.

For $\xi \gtrsim 2$ the pattern deviates from that for lower ξ. The factor in Eq. (18) appears to account for this, gradually shifting the time dependence from t_v to $\sqrt{t_u}$ as ξt_v increases and a diffusion-limited regime is approached.

The data interpretation makes use of the four non-NMR measurements, a, D, χ, ν, which are used only as the dephasing rate $\frac{1}{3}\chi\nu$, the diffusion time a^2/D, and their product ξ. The single-echo and CPMG data are interpreted in terms of four NMR-derived quantities (and the above non-NMR quantities): $\beta_v, T_{4u}, R_{sv}, T_{5w}$, all of them functions only of the *shape* of the pore structure. These are adequate to describe the effects of susceptibility differences and diffusion for our 18 sample and frequency combinations, with CPMG data as functions of τ, and with single-echo data as functions of $t = 2\tau$. We also discussed an exchange time $\tau_{eu} \gtrsim 16$ associated with the validity of the Cauchy distribution of phases for our smallest ξ value.

We were surprised to find that the distribution of phases for our porous porcelains approximates a truncated Cauchy distribution for the FID and for spin echoes. However, a number of systems of interest are known to produce truncated Cauchy distributions of magnetic fields, including dispersed magnetized particles [5,6] used as contrast agents in technologies as different as oil well logging and medical MRI. These systems can be scaled as described above. For particles that are ferromagnetic the magnetization can be substituted for $\chi\nu$, and grain radius or diameter can be the parameter a. The exchange time would presumably be related to the distance between particles. In any case our model and scaling laws are *not shape specific* except for dependence on the Cauchy distribution of fields. Any sources of dipole fields (either three dimensional or two dimensional) give a truncated Cauchy distribution of fields. One could have such fields from globules of one material, such as oil or fat or air, dispersed in another of different magnetic susceptibility and also from cylinders, such as blood vessels containing a contrast agent and subject to a transverse component of a magnetic field [29].

The additional transverse relaxation rate R from diffusion and susceptibility differences can be both a source of interference with measurements of transverse relaxation from other sources and also a possible source of useful information in porous media and of contrast in medical MRI. A knowledge of the scaling laws can be useful for both designing and interpreting NMR measurements.

ACKNOWLEDGMENTS

This research was partially supported by the Italian Consiglio Nazionale delle Richerche and Ministero dell'Università e della Richerca Scientifica. We thank M. Monduzzi (University of Cagliari, Italy) for measurements of diffusion coefficients and G. C. Cecchi (University of Ferrara, Italy) for measurement of the susceptibilities.

[1] E. L. Hahn, Phys. Rev. **80**, 580 (1950).
[2] H. Y. Carr and E. M. Purcell, Phys. Rev. **94**, 630 (1954).
[3] S. Meiboom and D. Gill, Rev. Sci. Instrum. **29**, 688 (1958).
[4] R. M. Weisskopf, C. S. Zuo, J. L. Boxerman, and B. R. Rosen, Magn. Reson. Med. **31**, 601 (1994).
[5] R. J. S. Brown, Magn. Reson. Med. **29**, 551 (1993).
[6] R. J. S. Brown, Phys. Rev. **121**, 1379 (1961).
[7] P. A. Hardy and R. M. Henkelman, Magn. Reson. Med. **17**, 348 (1991).
[8] R. N. Muller, P. Gillis, F. Moiny, and A. Roch, Magn. Reson. Med. **22**, 178 (1991).
[9] H. C. Torrey, Phys. Rev. **104**, 563 (1956).
[10] G. C. Borgia, R. J. S. Brown, P. Fantazzini, E. Mesini, and G. Valdrè, Nuovo Cimento D **14**, 745 (1992).
[11] R. J. S. Brown and P. Fantazzini, Phys. Rev. B **47**, 14 823 (1993).
[12] R. J. S. Brown and P. Fantazzini, Magn. Reson. Imag. **12**, 175 (1994).
[13] J. Zhong and J. C. Gore, Magn. Reson. Med. **19**, 276 (1991).
[14] R. L. Kleinberg and M. A. Horsfield, J. Magn. Reson. **88**, 9 (1990).
[15] S. Majumdar and J. C. Gore, J. Magn. Reson. **79**, 41 (1988).
[16] C. R. Fisel, J. L. Ackerman, R. B. Buxton, and T. J. Brady, Magn. Reson. Med. **17**, 336 (1991).
[17] P. Bendel, J. Magn. Reson. **86**, 509 (1990).
[18] P. T. Callaghan, J. Magn. Reson. **87**, 304 (1990).
[19] Y. Rozenman, X. Zou, and H. L. Kantor, Magn. Reson. Med. **14**, 31 (1990).
[20] P. Le Doussal and P. Sen, Phys. Rev. B **46**, 3465 (1992).
[21] G. E. Santyr, R. M. Henkelman, and M. J. Bronskill, J. Magn. Reson. **79**, 28 (1988).
[22] P. A. Hardy and R. M. Henkelman, Magn. Reson. Imag. **7**, 265 (1989).
[23] P. Gehr, J. D. Brain, S. B. Bloom, and P. A. Valberg, Nature (London) **302**, 336 (1983).
[24] R. L. Kleinberg, S. A. Farooqui, and M. A. Horsfield, J. Colloid Interface Sci. **158**, 195 (1993).
[25] Z. Taicher, G. Coates, Y. Gitarz, and L. Berman, Magn. Reson. Imag. **12**, 285 (1994).
[26] R. L. Kleinberg, A. Sezginer, D. D. Griffin, and M. Fukuhara, J. Magn. Reson. **97**, 466 (1992).
[27] G. C. Borgia, P. Fantazzini, G. Fanti, E. Mesini, L. Terzi, and G. Valdrè, Magn. Reson. Imag. **9**, 695 (1991).
[28] G. C. Borgia, A. Brancolini, R. J. S. Bronw, P. Fantazzini, and G. Ragazzini, Magn. Reson. Imag. **12**, 191 (1994).
[29] R. P. Kennan, J. Zhong, and J. C. Gore, Magn. Reson. Med. **31**, 9 (1994).